Vol. 80, No. 1

CD8+ T Cells Require Perforin To Clear West Nile Virus from Infected Neurons

Bimmi Shrestha,[1] Melanie A. Samuel,[2] and Michael S. Diamond[1,2,3]*

*Departments of Medicine,[1] Molecular Microbiology,[2] and Pathology & Immunology,[3]
Washington University School of Medicine, St. Louis, Missouri*

Injury to neurons after West Nile virus (WNV) infection is believed to occur because of viral and host immune-mediated effects. Previously, we demonstrated that CD8+ T cells are required for the resolution of WNV infection in the central nervous system (CNS). CD8+ T cells can control infection by producing antiviral cytokines (e.g., gamma interferon or tumor necrosis factor alpha) or by triggering death of infected cells through perforin- or Fas ligand-dependent pathways. Here, we directly evaluated the role of perforin in controlling infection of a lineage I New York isolate of WNV in mice. A genetic deficiency of perforin molecules resulted in higher viral burden in the CNS and increased mortality after WNV infection. In the few perforin-deficient mice that survived initial challenge, viral persistence was observed in the CNS for several weeks. CD8+ T cells required perforin to control WNV infection as adoptive transfer of WNV-primed wild-type but not perforin-deficient CD8+ T cells greatly reduced infection in the brain and spinal cord and enhanced survival of CD8-deficient mice. Analogous results were obtained when wild-type or perforin-deficient CD8+ T cells were added to congenic primary cortical neuron cultures. Taken together, our data suggest that despite the risk of immunopathogenesis, CD8+ T cells use a perforin-dependent mechanism to clear WNV from infected neurons.

West Nile virus (WNV) is a positive-sense single-stranded RNA virus of the family *Flaviviridae* and is related to other viruses that cause human disease including dengue, yellow fever, Japanese, St. Louis, and tick-borne encephalitis viruses. WNV is maintained in an enzootic cycle between mosquitoes and birds but also infects humans, horses, and other animals. It is endemic in parts of Africa, Europe, the Middle East, and Asia and has established its presence in North America. Humans develop a febrile illness, with a subset of cases progressing to meningitis, encephalitis, or a polio-like paralytic syndrome (1, 19, 33, 34).

After mosquito inoculation, initial WNV replication is believed to occur in skin dendritic cells, which migrate to draining lymph nodes (6, 20), where viral propagation and dissemination occur (18, 21, 35, 40, 66). After spread to the central nervous system (CNS), WNV infects and injures several different types of neurons, including those in the hippocampus, cerebellum, brain stem, cerebral cortex, and anterior horn of the spinal cord (8, 11, 56, 57, 67). In animals and humans, the maturation and integrity of the immune system correlate with resistance to WNV infection (1, 9, 11, 12, 14, 19, 33, 34, 58, 65).

Recent experiments with mice have provided insight into cell-mediated immune protection against WNV (9, 60). A strong CD8+ T-cell response is observed in the spleen within days of peripheral WNV infection (17, 24, 38, 63). CD8+ T cells contribute to the eradication of WNV as CD8-deficient or -depleted mice failed to clear virus from the CNS and had increased mortality (55, 63). A similar enhanced susceptibility was observed after infection with 10^2 to 10^3 PFU of WNV in

β_2-microglobulin-deficient or K^b- × D^b-deficient mice, which have severe deficits in their repertoire of antigen-restricted cytotoxic CD8+ T cells (46). Nonetheless, the mechanism of WNV clearance from infected neurons in the CNS remains unclear. CD8+ T cells could control neuronal infection through several independent mechanisms, including a class I major histocompatibility complex (MHC)-restricted and perforin-dependent cell death pathway or a Fas ligand-dependent cell death pathway, or through the production of antiviral cytokines such as gamma interferon (IFN-γ) or tumor necrosis factor alpha. Perforin-dependent control of virally infected target cells by activated CD8+ T and natural killer (NK) cells occurs through the granzyme-dependent granule exocytosis pathway, which results in programmed cell death (15, 50, 54).

To elucidate the mechanisms of CD8+ T-cell-mediated control of WNV infection, prior studies were performed with genetically deficient mice and the lineage II Sarafend strain of WNV (64). No change in mortality after infection was observed in mice that were genetically deficient in perforin, Fas, or Fas ligand. Compared to wild-type mice, equivalent virus titers were observed on days 10 and 13 after infection in the brains of perforin-, Fas-, or Fas ligand-deficient mice. Based on these data, Wang et al. concluded that perforin did not play a crucial role in the recovery from WNV infection, although higher viral burden and mortality were observed in perforin- × Fas ligand-deficient mice. Despite the apparent limited role of perforin in controlling Sarafend infection, increased mortality was observed in mice lacking granzymes A and B, suggesting a possible novel protective role of granzyme against WNV that was independent of perforin (64).

Although studies with the Sarafend strain provide insight as to how CD8+ T cells limit WNV infection, it is also important to evaluate how CD8+ T cells control infection by a lineage I North American strain. The lineage II Sarafend strain is dis-

* Corresponding author. Mailing address: Departments of Medicine, Molecular Microbiology, Pathology & Immunology, Washington University School of Medicine, 660 South Euclid Ave., Box 8051, St. Louis, MO 63110. Phone: (314) 362-2842. Fax: (314) 362-9230. E-mail: diamond@borcim.wustl.edu.

tinct genetically and functionally from the North American lineage I strains: the amino acid sequence identity ranges from 78% (capsid) to 95% (NS3), Sarafend has a unique binding pattern of neutralizing anti-E monoclonal antibodies (MAbs) (52), and Sarafend buds from the cell directly via the plasma membrane rather than through the Golgi-derived secretory pathway (45). Moreover, infection with a high (10^8 PFU) dose of the Sarafend strain resulted in greater mortality in wild-type compared to β_2-microglobulin-deficient mice, suggesting that under some conditions, $CD8^+$ T cells contribute to immunopathogenesis and disease (63).

In the present study, we directly assessed the role of perforin in $CD8^+$ T-cell clearance of viral infection in the CNS in mice with a lineage I North American WNV strain (isolated in New York in 2000). We found that a genetic deficiency of perforin resulted in increased CNS WNV burden and mortality. Antibody depletion and adoptive transfer experiments established that $CD8^+$ T cells require perforin to clear WNV infection from neurons in vitro and in vivo.

MATERIALS AND METHODS

Viruses. The WNV strain (3000.0259) isolated in New York in 2000 (hereafter, New York 2000 strain) was used as described earlier (55). The stock virus (2×10^8 PFU/ml) was propagated once in C6/36 *Aedes albopictus* cells and used for all in vivo and in vitro studies.

Mouse experiments and tissue preparation. C57BL/6 (H-$2K^b$) inbred wild-type mice were obtained from a commercial vendor (Jackson Laboratories, Bar Harbor, ME). The congenic perforin-, IFN-γ-, CD8α-, and K^b- $\times$ D^b-deficient mice were obtained as gifts (perforin deficient, T. Ley, Washington University School of Medicine; CD8 deficient and IFN-γ deficient, H. Virgin, Washington University School of Medicine; and K^b- $\times$ D^b-deficient, T. Hansen, Washington University School of Medicine). All mice were genotyped, bred, and handled in the animal facility of Washington University School of Medicine in accordance with institutional policy. Eight- to 12-week-old adult mice were used for all studies and were inoculated with 10^2 PFU of WNV by footpad injection. For immunohistochemistry, brains from moribund mice were harvested after perfusion with 10 ml of phosphate-buffered saline (PBS) and 4% paraformaldehyde on day 10 after infection. Tissues were fixed in 4% paraformaldehyde for 24 h at 4°C, washed into PBS, and subsequently embedded in paraffin. Brains were sectioned and stained for WNV antigen and leukocyte common antigen (CD45) by immunohistochemistry as previously described (55). Briefly, paraffin-embedded brain sections were dewaxed and then digested with a protease enzyme derived from *Streptomyces griseus* (Sigma Chemical, St. Louis, MO), and endogenous peroxidase activity was quenched with 0.3% H$_2$O$_2$. After incubation with blocking solution, diluted WNV immune or nonimmune rat serum or anti-CD45 monoclonal antibody (BD Pharmingen) was added for 1 h at room temperature. Sections were then incubated with biotinylated goat anti-rat or anti-mouse antibody followed by horseradish peroxidase-conjugated avidin-biotin complex (Vector Laboratories). Positive signal was visualized with diaminobenzidine, and hematoxylin was used as a counterstain.

Brain T-cell isolation. Perforin-deficient and wild-type mice were infected with 10^2 PFU by footpad injection, and on day 10 after infection, mice were anesthetized and perfused extensively with 30 ml of PBS. Individual brains were harvested, kept on ice in RPMI supplemented with 5% fetal bovine serum (FBS), and homogenized gently by pressing through a 100-μm-mesh tissue strainer (BD Pharmingen, San Diego, CA). The cell homogenates were centrifuged, and the cell pellets were resuspended in RPMI and overlaid on a 70% and 30% Percoll (Pharmacia, Uppsala, Sweden) step gradient in RPMI. The gradients were centrifuged (800 $\times$ g for 25 min at 25°C), and the leukocytes were collected from between the 70% and 30% interface. Leukocytes were washed twice, incubated with Fcγ receptor block (BD Pharmingen), and stained for CD4$^+$ and CD8$^+$ T cells with fluorescein isothiocyanate (FITC)-conjugated CD4 (L3T4) or CD8α (Ly-2) antibodies (BD Pharmingen) for 30 min at 4°C in the presence of 5% goat serum. After washing, cells were fixed with 1% paraformaldehyde in PBS and analyzed by flow cytometry (FACscan, Becton Dickinson, San Jose, Calif.) with CellQuest software. The total number of CD4$^+$ or CD8$^+$ T cells from each brain was determined by multiplying the percentage of CD4$^+$ or CD8$^+$ T cells by the total number of leukocytes harvested.

Quantitation of virus burden in tissues. To analyze the kinetics of viral burden in tissues, mice were infected with 10^2 PFU by footpad injection and sacrificed on day 2, 4, 6, 8, or 10 after infection. Before harvesting organs, blood was collected from the axillary vein by phlebotomy. After extensive perfusion with PBS, organs were removed and homogenized using a Bead-Beater apparatus and viral plaque assays were performed as previously described (55).

Intracellular IFN-γ staining. Intracellular IFN-γ staining of wild-type and perforin-deficient splenocytes was performed as described previously (61). Briefly, at day 7 after infection, splenocytes were harvested from wild-type and perforin-deficient mice. Erythrocytes were lysed with ACK lysis buffer, and splenocytes were counted. In a 96-well plate, 10^6 splenocytes were either left untreated or stimulated with 50 ng/ml phorbol myristate acid (Sigma Chemical) and 500 ng/ml ionomycin (Sigma Chemical) for 10 min. Subsequently, Golgi plug (BD Pharmingen) was added and incubated for 4 h at 37°C in Dulbecco's modified Eagle's medium (DMEM) supplemented with 10% FBS. Cells were harvested and stained with FITC-conjugated anti-CD8 (Ly-2) antibody (BD Pharmingen) for 30 min at 4°C. Cells were fixed in 4% paraformaldehyde and permeabilized with 0.5% saponin, incubated with Fcγ receptor block (BD Pharmingen), and stained with AlexaFluor 647-conjugated rat anti-mouse IFN-γ antibody (BD Pharmingen) or rat immunoglobulin G1 (IgG1) (isotype control) for 30 min at 4°C. After washing and fixing, cells were analyzed by flow cytometry.

Adoptive transfer experiments. To obtain WNV-primed CD8$^+$ T cells, splenocytes were harvested from naïve or WNV-infected wild-type, perforin-deficient, or IFN-γ-deficient mice at day 7 after infection. CD8$^+$ T cells were isolated by negative selection using antibody-coated magnetic beads (Miltenyi Biotec, Auburn, CA), and purity ($\geq$95% CD8$^+$ T cells) was confirmed by flow cytometry using an FITC-conjugated rat anti-mouse CD8 antibody. Wild-type, perforin-deficient, or IFN-γ-deficient CD8$^+$ T cells were adoptively transferred by intraperitoneal inoculation into CD8-deficient or K^b- $\times$ D^b-deficient mice 24 h after subcutaneous WNV infection. In some experiments, survival analysis was performed, while in others, mice were euthanized at day 10 after infection for analysis of viral burden in the spleen, brain, and spinal cord.

Antibody depletion of natural killer cells. Natural killer cells were depleted in wild-type C57BL/6 mice using the PK136 hybridoma (IgG2a) against the mouse NK1.1 antigen (gift of W. Yokoyama, Washington University, St. Louis, MO). The antibody was cultured in roller bottles, concentrated, and purified by protein G affinity chromatography according to the manufacturer's instructions (Pharmacia). An anti-severe acute respiratory syndrome (SARS) virus antibody (2E11, anti-open reading frame 7a [ORF7a]; IgG2a) (44) was produced, purified, and used as an isotype control for these studies. After purification, 100 μg of anti-NK1.1 or control anti-ORF7a was administered via the intraperitoneal route at days -2 and $+2$ with respect to WNV infection. The depletion of natural killer cells was confirmed by flow cytometry after staining peripheral blood mononuclear cells with an anti-CD49b antibody (clone DX5; BD Pharmingen).

Antibody depletion of CD8$^+$ T cells. CD8$^+$ T cells were depleted with a rat monoclonal antibody (H35; rat IgG2b) specific for mouse CD8$^+$ T cells according to a previously published protocol (41). A hybridoma (SFR33; rat IgG2b) that produced antibodies against human HLA-DR5 molecules was grown in parallel and used as a negative isotype control. H35 and SFR33 were grown in a serum-free medium in 1-liter bioreactor flasks according to the manufacturer's instruction (Integra Biosciences, Ijamsville, MD). The supernatants were harvested, centrifuged, filtered, and quantitated by enzyme-linked immunosorbent assay. As a control, to confirm that the CD8$^+$ T cells conferred protection, antibody depletion studies were combined with adoptive transfer studies. Anti-CD8 or HLA-DR MAbs (500 μg) were administered to CD8-deficient mice via the intraperitoneal route 2 days prior to adoptive transfer of CD8$^+$ T cells. This dose of MAb was previously shown to deplete CD8$^+$ T cells from wild-type C57BL/6 mice by greater than 99% (41). One day after adoptive transfer, the efficiency of antibody depletion of CD8$^+$ T cells was assessed by flow cytometry after staining peripheral blood mononuclear cells with a phycoerythrin-conjugated anti-CD8 MAb (clone 53-6.7; BD Pharmingen) that recognized a distinct epitope.

Addition of CD8$^+$ T cells to WNV-infected neurons. Primary neuronal cultures were established from the cortical hemispheres of the brain from day 15 embryos of wild-type C57BL/6 mice as previously described (30, 68). Briefly, the embryos were harvested at day 15 after gestation and the brains were removed and placed in a 35-mm dish with DMEM on ice. The cortical hemispheres were separated, placed in a 15-ml tube in DMEM, and centrifuged at 300 rpm for 5 min at 4°C. The cells were incubated with 1 ml of 0.25% trypsin (Sigma Chemical) and 300 μl of DNase I (Invitrogen, Carlsbad, Calif.) for 15 min at room temperature. The cells were washed with DMEM supplemented with 20% FBS, resuspended, and passed through a 70-μm cell strainer (Fisher Scientific). After counting, cortical

neurons were plated (6×10^5 cells/well) on poly-D-lysine- and laminin (BD Biosciences)-coated coverslips in a 24-well plate and incubated at 37°C for 24 h. After 24 h, the medium was replaced with neurobasal medium supplemented with B-27 (Invitrogen, Carlsbad, Calif.) for the enrichment of neurons (56). Three to 4 days after plating, neurons were infected with WNV at a multiplicity of infection (MOI) of 0.001 for 1 h. After removing unbound virus with four washes of warm medium, purified naive or WNV-primed CD8$^+$ T cells from wild-type or perforin-deficient mice were added at 10:1 or 80:1 effector/target (E:T) ratios. Supernatants were harvested at 48 h after infection, and WNV production was measured by plaque assay.

Cortical neurons were phenotyped for their purity and degree of infection as follows. Neurons were infected at an MOI of 0.001 and 48 h later fixed with 4% paraformaldehyde in PBS at 4°C. Cells were permeabilized and blocked (0.05% Triton X-100, 5% normal goat serum, and 3% bovine serum albumin in PBS) for 1 h at room temperature. Cells were stained with the neuron-specific marker rabbit anti-MAP2 (42) (Chemicon International, Temecula, CA) or normal rabbit IgG for 1 h at room temperature. After four washes with PBS, neurons were costained with rat anti-WNV immune serum or normal rat serum for 1 h at room temperature. After four washes with PBS, positive signals were detected using Cy3-conjugated anti-rat (Jackson Laboratories, West Grove, PA) and Alexa-488-conjugated anti-rabbit secondary antibodies (Molecular Probes Inc., Eugene, OR). After counterstaining with diamidino-4′,6′-phenylindole (DAPI), neurons were visualized by fluorescence microscopy (Zeiss Axiovert 200, Oberkochen, Germany).

Data analysis. All data were analyzed statistically using Prism software (GraphPad, San Diego, CA). For in vitro experiments, an unpaired t test was used to determine significant differences. Kaplan-Meier survival curves were analyzed by the log-rank test. Differences in viral burden were analyzed by the Mann-Whitney test.

RESULTS

Susceptibility of perforin-deficient mice to WNV infection. Previously, we and others have demonstrated that a deficiency of CD8$^+$ T cells in mice resulted in substantially higher levels of infectious WNV in the CNS with increased mortality (55, 63). Since CD8$^+$ T cells control other viral infections by both cytolytic and noncytolytic mechanisms, we assessed the role of perforin in the control of WNV infection. Because WNV predominantly infects neurons in the CNS, perforin-dependent neuronal death could have a protective and/or pathogenic effect (63). To assess the net effect of perforin on WNV infection and disease, we compared survival rates of wild-type and congenic perforin-deficient C57BL/6 mice after infection. After subcutaneous inoculation with 10^2 PFU of a virulent WNV strain from New York, within 8 days, mice showed clinical signs of infection, including reduced activity, weight loss, hair ruffling, and hunchback posture. However, survival rates were markedly lower in perforin-deficient mice: 22% compared to 70% in congenic wild-type mice (Fig. 1A; $P < 0.0001$). Moreover, similar to CD8-deficient mice (55), we observed an increased incidence of severe neurological signs, including hemiplegia, tremor, and seizure in perforin-deficient mice. By morbidity and mortality analyses, an absence of perforin caused more severe WNV infection with adverse clinical outcomes.

WNV burden in perforin-deficient mice. To understand how a deficiency of perforin resulted in increased susceptibility to WNV infection, the level of infectious virus in peripheral and CNS tissues was determined by viral plaque assay in BHK21 cells. Wild-type and perforin-deficient mice were infected with 10^2 PFU, and viral load was measured at days 2, 4, 6, 8, and 10 after infection in the serum, spleen, brain, and spinal cord (Fig. 1B to D).

(i) Viremia. In both wild-type and perforin-deficient mice, viremia was undetectable by viral plaque assay throughout the time course, results that are consistent with our previous pub-

lications (10, 55). Viral RNA was thus measured in serum using a more sensitive fluorogenic reverse transcription-PCR assay (32). The kinetics and magnitude of viremia were virtually identical between wild-type and perforin-deficient mice; viral RNA was detected from day 2 to day 4 after infection but was cleared from circulation by day 6 (data not shown). These results were similar to that previously obtained with CD8-deficient mice (55).

(ii) Spleen. Infectious virus was detected in the spleens both groups at 4 days after infection. However, in wild-type mice, only 40% (2/5) of mice had levels above the limit of sensitivity. In contrast, 100% (5/5) of perforin-deficient mice had measurable virus ($\sim 10^4$ PFU/g) in the spleen. Subsequently, in the wild-type mice, infectious WNV levels decreased by day 6 and were absent at day 8. In contrast, there was an attenuated clearance phase in the perforin-deficient mice as levels of virus (10^3 PFU/g) persisted in the spleen after day 6 (Fig. 1B). At days 8 and 10, 90% (9/10) and 40% (4/10) of perforin-deficient mice had detectable infectious WNV, respectively. Thus, compared to wild-type controls, a lack of perforin resulted in a failure to rapidly clear virus infection from the spleen.

(iii) CNS. (a) Spinal cord. WNV was detected earlier and in greater levels in the spinal cord of perforin-deficient mice (Fig. 1C). At day 6 after infection, 75% (6/8) of perforin-deficient mice had detectable ($\sim 10^4$-10^5 PFU/g) levels in the spinal cord (Fig. 1C). In contrast, infectious virus was not detected in wild-type mice until 8 days after infection. By the latter stages of the time course, the magnitude of viral infection in the spinal cord was markedly increased in perforin-deficient mice. At day 10, ~ 70-fold higher levels ($P < 0.02$) of WNV were detected in the spinal cord of perforin-deficient mice.

(b) Brain. A slightly different pattern of infection was observed in the brain (Fig. 1D). Earlier entry into the brain was not observed in perforin-deficient mice. However, there was a statistically significant ($10^{4.5}$ PFU/g versus $10^{3.3}$ PFU/g; $P < 0.01$) increase in viral burden at day 6 in perforin-deficient mice. As the time course progressed, the gap in viral burden in the brain widened such that by day 10 after infection there were ~ 60-fold-higher levels ($P < 0.02$) of infectious virus in the perforin-deficient mice. Overall, the virologic analysis demonstrates that perforin has an essential role in controlling the levels of WNV infection in the CNS.

Delayed clearance of WNV from the CNS of surviving perforin-deficient mice. Previously, we showed that a lack of CD8$^+$ T cells resulted in WNV persistence in the CNS in the few surviving CD8-deficient mice up to 5 weeks after infection (55). Analogously, infection of perforin-deficient mice resulted in a small (~ 22%) number of surviving animals. To assess the effect of perforin on the kinetics of CNS viral clearance, levels of infectious virus in the CNS were measured in the surviving wild-type and perforin-deficient mice (Fig. 1E). In wild-type mice, no infectious virus was detected in the brain after 21 days. In contrast, similar to that observed with CD8-deficient mice (55), significant levels (10^3 PFU/gm) of WNV were detected in perforin-deficient mice at later times. Even 35 days after infection, 10^2 PFU/g infectious WNV was recovered from 67% of the brains of perforin-deficient mice. Thus, an absence of CD8$^+$ T cells (55) or perforin molecules resulted in delayed clearance of WNV from infected cells in the CNS.
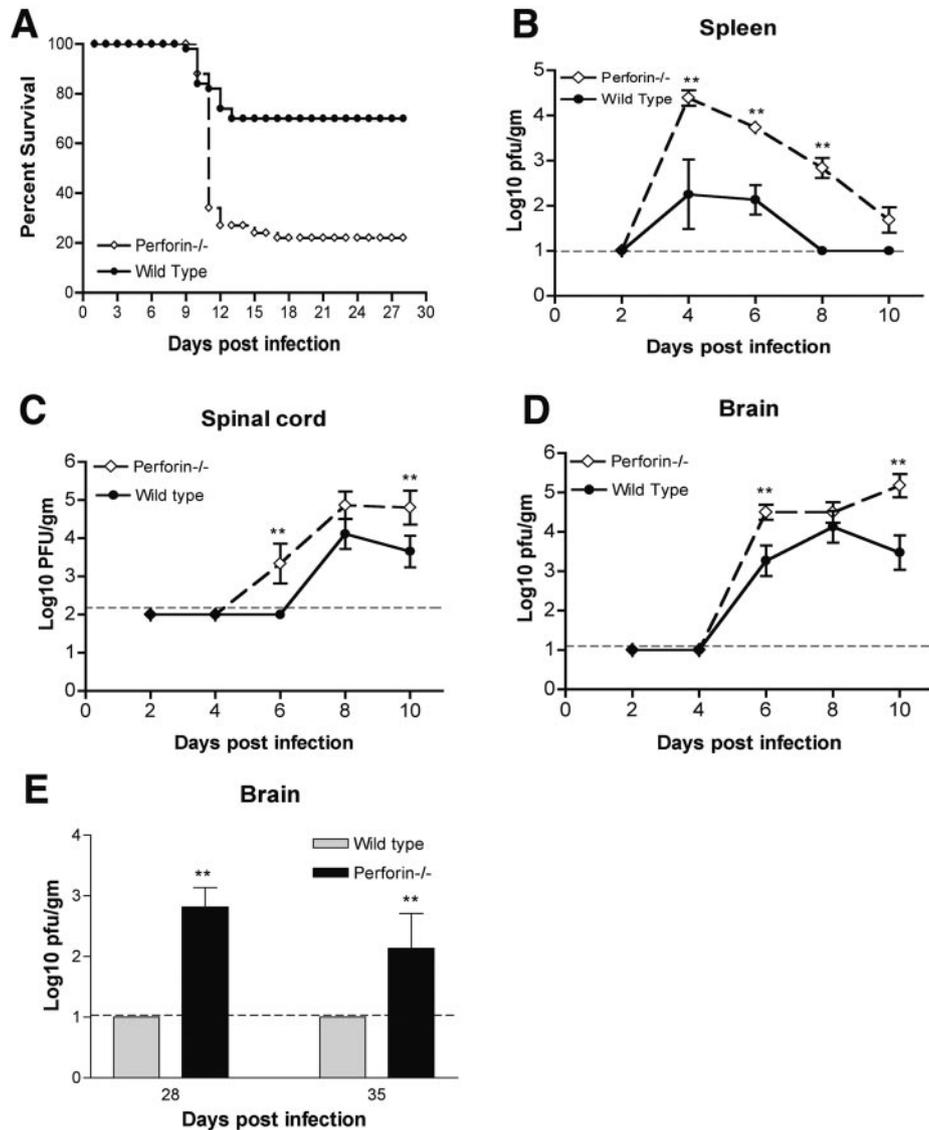
FIG. 1. Survival and viral load analysis for wild-type and perforin-deficient C57BL/6 mice inoculated with 10^2 PFU of WNV. (A) Wild-type and perforin-deficient mice were inoculated with WNV and monitored for morbidity and mortality for 28 days. The numbers of animals were $n = 50$ for wild-type mice and $n = 41$ for perforin-deficient mice. Survival differences were statistically significant ($P < 0.0001$). (B to E) WNV tissue burden. Infectious WNV levels were measured from the (B) spleen, (C) spinal cord, and (D) brain of wild-type and perforin-deficient mice using a viral plaque assay in BHK21 cells after tissues were harvested at the indicated days. Data are shown as the average PFU per gram of tissue and reflect 5 to 10 mice per time point for either wild-type or perforin-deficient mice. (E) Persistent WNV infection in the brain of surviving wild-type and perforin-deficient mice as determined by plaque assay. For all viral burden experiments, the dotted line represents the limit of sensitivity of viral detection and asterisks denote statistically significant ($P < 0.05$) differences between wild-type and perforin-deficient mice.

Increased neuronal infection in the CNS of perforin-deficient mice after WNV infection. Because there were higher viral titers in the CNS of perforin-deficient mice at day 10 after infection, we evaluated whether there was a difference in the susceptibility of different neuronal populations to WNV infection. Similar to that previously observed (55, 56), WNV antigen was detected only in neurons (Fig. 2) (data not shown). The cortex, brain stem, cerebellum, and base of the brain were the principal sites of WNV infection in the brain. However, compared to comparably sickened wild-type mice at day 10 after infection, more intense viral antigen staining and greater numbers of infected neurons were observed in perforin-defi-

cient mice. Many of the heavily infected neurons in the perforin-deficient mice showed evidence of neuronal injury with altered morphology (Fig. 2, red arrows). Similarly, in the spinal cord, larger numbers of neurons were infected in perforin-deficient mice when compared to equivalently sickened wild-type mice. Thus, an absence of perforin granules resulted in increased CNS viral load because of enhanced infection in neurons throughout the brain and spinal cord.

CNS inflammation in perforin-deficient mice. In prior studies (55, 56), we observed large numbers of CD45+ lymphocytes in the brains of mice infected with WNV, and that the entrance of these cells temporally correlated with clearance of virus

from infected neurons. To confirm that the increased viral load in the brains of perforin-deficient mice was not due to a significant change in CNS inflammation, we assessed the number of CD45^{+} leukocytes in the brains of wild-type and perforin-deficient mice on day 10 after infection by immunohistochemistry. Although leukocytes were present throughout the brain, the largest concentration of CD45^{+} cells in wild-type or perforin-deficient mice was observed in the brain stem (data not shown). As expected, a deficiency of perforin did not significantly alter the number or pattern of inflammatory cells in the brain (Fig. 3A; $P > 0.1$) (data not shown). Thus, the increased viral load in the CNS associated with perforin deficiency was not due to a dramatic difference in the number of leukocytes within the CNS.

Previously, we showed that CD8^{+} T cells traffic into the brain after viral infection in wild-type mice and that this event was temporally associated with reductions in viral titers (55). As an additional control, we confirmed that perforin-deficient mice had normal trafficking of CD8^{+} T cells into the brain. Leukocytes from the brains of wild-type and perforin-deficient mice were isolated by Percoll gradient centrifugation on day 10 after infection and phenotyped by flow cytometry. No significant differences in trafficking of CD8^{+} or CD4^{+} T cells into the brain were observed in perforin-deficient mice (Fig. 3B; $n = 9$, $P \geq 0.7$). Thus, the delayed and inefficient CNS clearance of WNV infection in perforin-deficient mice was not due to decreased migration of T cells. We also assessed whether the absence of perforin had an effect on the priming of CD8^{+} T cells by comparing levels of IFN-γ secretion after ex vivo stimulation. Splenocytes from wild-type or perforin-deficient mice were harvested at day 7 after WNV infection. After stimulation with phorbol ester and ionomycin, CD8^{+} T cells were analyzed by flow cytometry for intracellular IFN-γ expression. Although infection with WNV resulted in a significant increase in the percentage and number of IFN-γ-producing CD8^{+} T cells ($P < 0.05$) compared to uninfected mice (Fig. 3C) (data not shown), no difference was observed between infected wild-type and perforin-deficient mice at day 7 after infection ($P = 0.7$). Collectively, these experiments suggest that the higher levels of WNV infection in the CNS of perforin-deficient mice were not due to a defect in activation or migration of CD8^{+} T cells.

WNV burden after adoptive transfer of wild-type and perforin-deficient CD8^{+} T cells. To directly establish the role of perforin in CD8^{+} T-cell-mediated protection of WNV infection, we performed adoptive transfer studies with WNV-primed perforin-sufficient or -deficient CD8^{+} T cells. To generate WNV-primed CD8^{+} T cells, wild-type or perforin-deficient C57BL/6 mice were infected with WNV, and on day 7, spleens were harvested and CD8^{+} T cells were purified by negative selection to greater than 95% purity using antibody-coated magnetic beads (data not shown). These cells were adoptively transferred into congenic CD8-deficient mice 1 day after WNV infection, and 9 days later (day 10 after infection), tissues were harvested to evaluate the effect on clearance of WNV infection in the periphery and CNS (Fig. 4). As previously observed (55), without adoptive transfer CD8-deficient mice had sustained viral burden in the spleen ($\sim 10^4$ PFU/g) and high viral loads in the brain (data not shown). When wild-type naïve CD8^{+} T cells (10×10^6) were transferred to CD8-deficient mice, no signif-
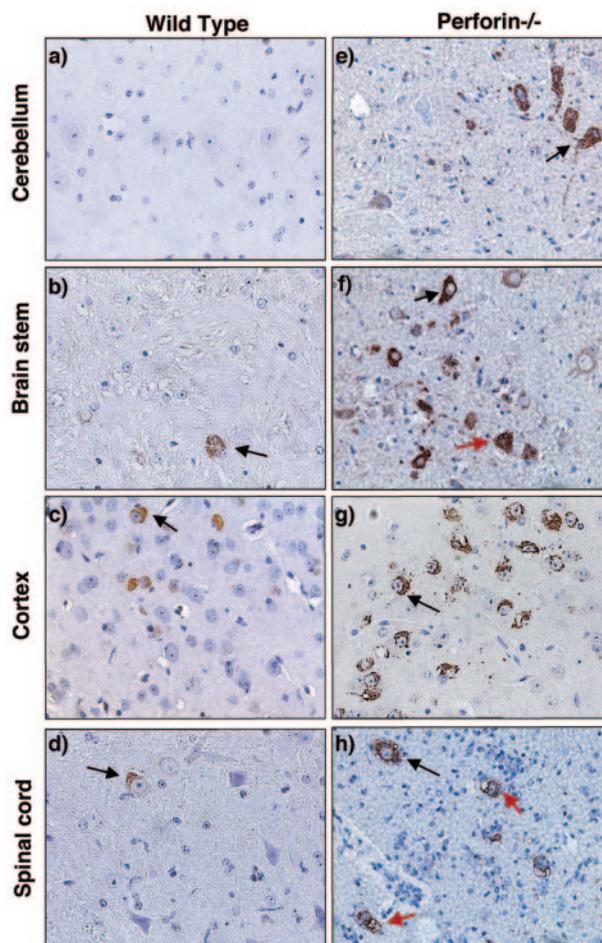

FIG. 2. Detection of WNV antigen in the brains of infected wild-type and perforin-deficient mice by immunohistochemistry. Brains from equivalently moribund wild-type (a to d) and perforin-deficient (e to h) mice were harvested at day 10 after infection with 10^2 PFU of WNV, sectioned, and stained for WNV antigen. Examples of infected cells or injured neurons are indicated with black and red arrows, respectively. Typical sections are shown from the cerebellum (a and e), brain stem (b and f), cerebral cortex (c and g), and spinal cord (d and h) after review of more than 10 independent brains from either wild-type or perforin-deficient mice.

icant clearance in the spleen or CNS was observed by day 10 (Fig. 4A). However, when wild-type or IFN-γ-deficient WNV-primed CD8^{+} T cells (10×10^6) were transferred, WNV was completely cleared from the spleen, brain, and spinal cord (Fig. 4A and G). In contrast, transfer of 10×10^6 perforin-deficient WNV-primed CD8^{+} T cells to CD8-deficient mice cleared infection from only 33% of spleen and CNS tissues (Fig. 4B). The remaining mice averaged $\sim 5 \times 10^2$ PFU/g in the spleen and $\sim 10^3$ to 10^5 PFU/g in the spinal cord and brain. Survival analysis that was performed in parallel supported these results, as adoptive transfer of wild-type WNV-primed CD8^{+} T cells provided superior protection compared to perforin-deficient CD8^{+} T cells (Fig. 4C, wild type, 93% survival; perforin deficient, 50% survival; $P = 0.01$). To confirm that the transferred CD8^{+} T cells mediated the protection, antibody depletion studies were performed. CD8-deficient mice that received anti-CD8 antibody prior to and after adoptive transfer
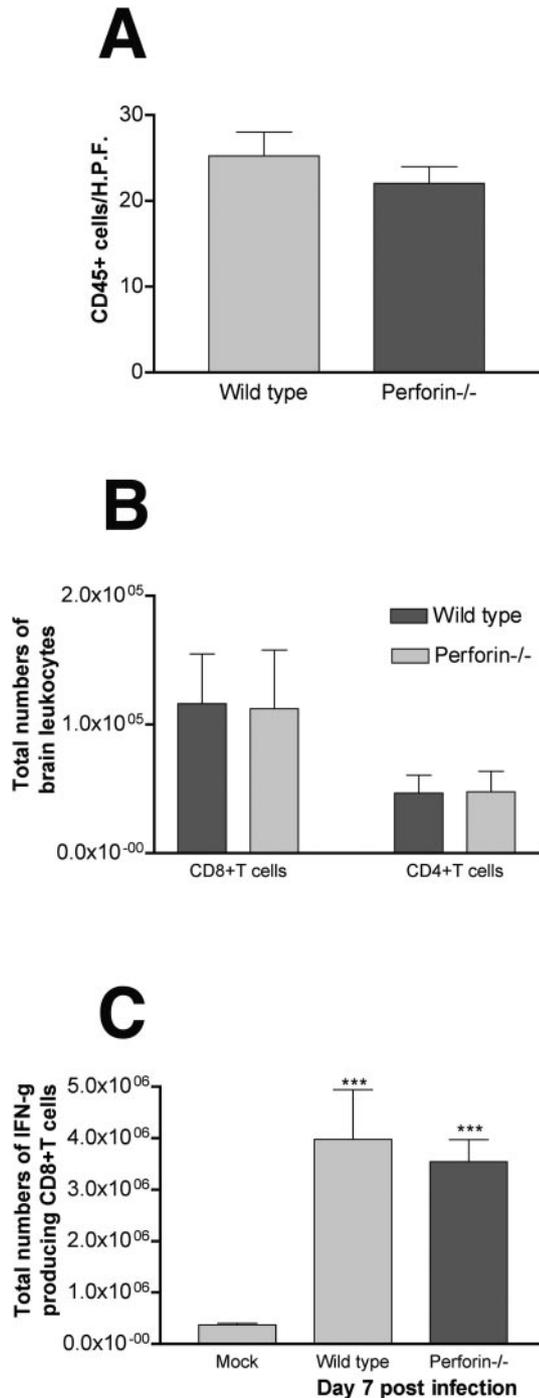
FIG. 3. Characterization of perforin-deficient CD8^{+} T cells. (A) Levels of CD45^{+} inflammatory cells in the brains of wild-type and perforin-deficient mice. Brain sections from wild-type and perforin-deficient mice at day 10 after infection were stained with rat anti-mouse CD45 antibody. The number of CD45^{+} cells per high-power field was counted from 10 independent fields from each mouse. No significant difference was observed ($P > 0.1$). (B) Migration of CD8^{+} and CD4^{+} T cells into the brains of WNV-infected mice. Wild-type and perforin-deficient mice ($n = 9$ per group) were infected with 10^2 PFU of WNV. At day 10, brain leukocytes were isolated by Percoll gradient centrifugation and phenotyped with phycoerythrin-conjugated anti-CD8 or anti-CD4 antibodies. The data are expressed as average numbers of CD8^{+} or CD4^{+} T cells and reflect the total number of brain leukocytes recovered after Percoll gradient centrifugation multiplied by the percentage that expressed CD8α (Ly-2) chain or CD4 antigen as measured by flow cytometry. No significant difference was observed ($P = 0.9$). (C) Intracellular staining of IFN-γ production by CD8^{+} T cells in the spleens of WNV-infected mice. Wild-type and perforin-deficient mice ($n = 8$ per group) were infected with 10^2 PFU of WNV. At day 7 after infection, splenocytes were harvested and left untreated (Mock) or stimulated ex vivo with phorbol ester and ionomycin for 4 h. Cells were then stained with FITC-conjugated anti-CD8 antibody and Alexa 647-conjugated anti IFN-γ antibody and analyzed by flow cytometry. The data are expressed as average numbers of CD8^{+} T cells producing IFN-γ. Asterisks indicate differences that are significantly different compared to mock-treated cells ($P \leq 0.05$). No difference in IFN-γ expression was observed between wild-type and perforin-deficient CD8^{+} T cells ($P = 0.7$).
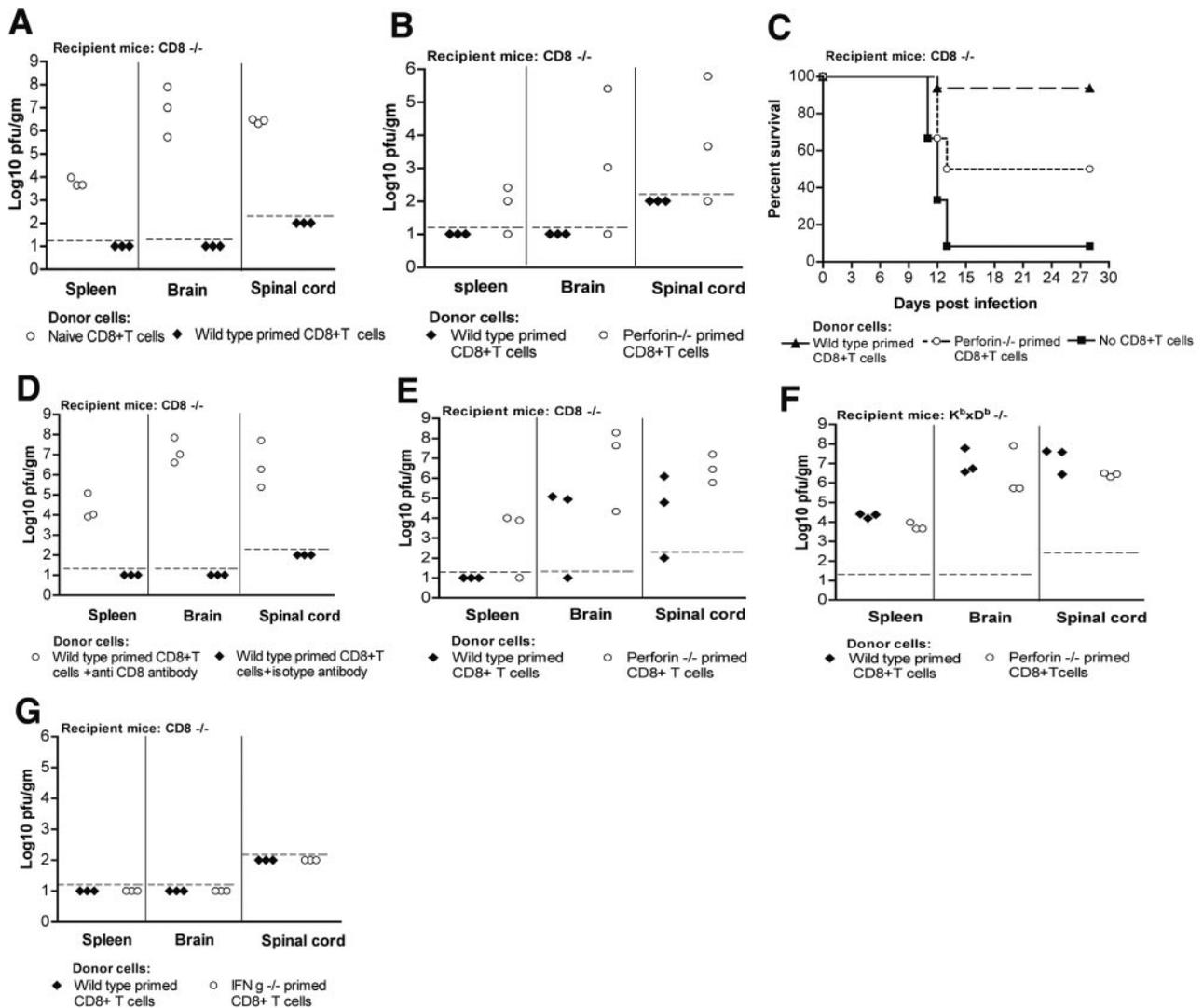
of WNV-primed wild-type CD8^{+} T cells showed no virologic improvement or enhanced survival (Fig. 4D) (data not shown).

Although transfer of 10×10^6 WNV-primed wild-type but not perforin-deficient CD8^{+} T cells resulted in no detectable virus at day 10 after infection, we were concerned that this high dose of primed T cells may have controlled infection in the periphery such that WNV did not disseminate to the brain. To clarify the role of perforin in CD8^{+} T-cell clearance in the CNS, fewer (3×10^6) WNV-primed CD8^{+} T cells were also transferred (Fig. 4E). When 3×10^6 wild-type WNV-primed CD8^{+} T cells were transferred to CD8-deficient mice, WNV was cleared completely from the spleen but not from the CNS as 67% of mice had reduced but measurable levels ($\sim 10^5$ to 10^6 PFU/g) in the brain and spinal cord. In contrast, transfer of 3×10^6 perforin-deficient WNV-primed CD8^{+} T cells failed to clear WNV from the spleen in 67% of recipient mice. Moreover, none of these recipient mice cleared infection from the CNS and viral titers approached that of CD8-deficient mice (10^7 to 10^8 PFU/g) (55) in several of the animals (Fig. 4E).

Adoptive transfer of CD8^{+} T cells into K^b- × D^b-deficient mice. The adoptive transfer studies with CD8-deficient mice suggested that CD8^{+} T cells clear WNV infection from the CNS through a perforin-dependent mechanism. Although most neurons do not express class I MHC molecules under basal conditions, inflammatory stimuli may increase class I MHC expression in certain subpopulations of neurons in vivo (31, 43). To directly assess whether the perforin-dependent clearance of viral infection by CD8^{+} T cells was also class I MHC dependent, WNV-primed CD8^{+} T cells were transferred into recipient class I MHC K^b- × D^b-deficient mice. Interestingly, transfer of 10×10^6 wild-type or perforin-deficient CD8^{+} T cells to K^b- × D^b-deficient mice failed to clear WNV from the spleen, brain, or spinal cord by day 10 after infection (Fig. 4F). Thus, CD8^{+} T cells clear WNV in a perforin-dependent, antigen-restricted manner both in the periphery and in the CNS.

Role of natural killer cells in WNV infection. Since natural killer (NK) cells also utilize perforin for target cell cytolysis, we examined their contribution to the clearance of WNV infection. NK cells were depleted from wild-type C57BL/6 mice using an antibody against the NK1.1 antigen. After two 100-μg doses, few ($\leq 0.1\%$) NK cells were detected in peripheral blood (Fig. 5A). Notably, mice that were treated with an anti-NK 1.1 or isotype control antibody and then infected with WNV showed no difference in morbidity, mortality, or viral load (Fig. 5B) (data not shown). Thus, at least for WNV infection in

FIG. 4. WNV infection after adoptive transfer of naïve or WNV-primed CD8$^+$ T cells. CD8$^+$ T cells were purified from naïve or WNV-primed wild-type, IFN-γ-deficient, or perforin-deficient mice and transferred 24 h after infection into CD8-deficient (A, B, C, D, E, and G) or $K^b \times D^b$ class I MHC-deficient (F) mice. (A) Viral burden at day 10 after adoptive transfer into CD8-deficient mice of 10×10^6 CD8$^+$ T cells from naïve and WNV-primed wild-type mice. (B) Viral burden at day 10 after adoptive transfer into CD8-deficient mice of 10×10^6 CD8$^+$ T cells from WNV-primed wild-type or perforin-deficient mice. (C) Survival curve of CD8-deficient mice after adoptive transfer of WNV-primed wild-type or perforin-deficient CD8$^+$ T cells at 24 h postinfection. The number of mice was 12 to 14 for each arm, and the survival difference between adoptive transfer of primed wild-type and perforin-deficient CD8$^+$ T cells was statistically significant ($P = 0.01$). (D) Effect of depletion of CD8$^+$ T cells with an anti-CD8 or isotype control antibody after adoptive transfer of CD8$^+$ T cells to CD8-deficient mice. (E) Viral burden at day 10 after adoptive transfer of 3×10^6 WNV-primed wild-type or perforin-deficient CD8$^+$ T cells into CD8-deficient mice. (F) Viral burden at day 10 after adoptive transfer of 10×10^6 WNV-primed wild-type or perforin-deficient CD8$^+$ T cells into $K^b \times D^b$ class I MHC-deficient mice. (G) Viral burden at day 10 after adoptive transfer of 10×10^6 WNV-primed wild-type or IFN-γ-deficient CD8$^+$ T cells into CD8-deficient mice.

mice, NK cells did not appear to have a primary role in controlling infection and disease.

Addition of wild-type and perforin-deficient CD8$^+$ T cells to WNV-infected neurons. To directly establish that CD8$^+$ T cells were necessary and sufficient for viral clearance from WNV-infected neurons, we developed a viral clearance assay with primary neurons derived from the cerebral cortex of 15-day-old wild-type C57BL/6 mouse embryos. Using antibodies against the neuron-specific marker MAP2 (42) and WNV, we confirmed that the cortical neuron cultures were comprised of >90% neurons and infected (Fig. 6A). One hour after infec-

tion, WNV-primed wild-type or perforin-deficient CD8$^+$ T cells were added at two different E:T ratios. At 48 h after infection, the level of infectious virus in the neuronal supernatants was measured by plaque assay. As expected, wild-type WNV-primed but not naïve CD8$^+$ T cells significantly reduced (~300-fold, $P < 0.0001$) infectious virus production from infected cortical neurons at both high and low E:T ratios (Fig. 6B). Although WNV-primed perforin-deficient CD8$^+$ T cells reduced virus production in cortical neurons compared to naïve CD8$^+$ T cells, they were ~30-fold less efficient ($P \leq 0.03$) than WNV-primed wild-type CD8$^+$ T cells at either E:T ratio.
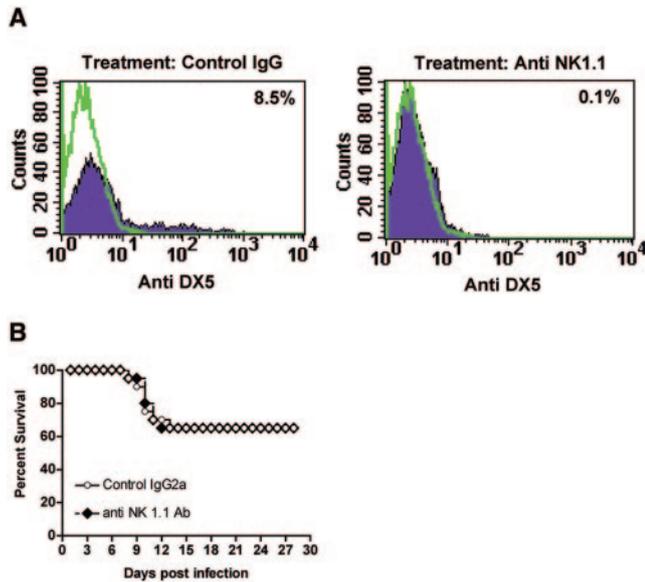
FIG. 5. Survival of wild-type mice with WNV infection after depletion of natural killer cells. Natural killer cells were depleted from wild-type mice after treatment with anti-NK1.1 antibody 2 days before and after infection with WNV. (A) Depletion of NK cells was confirmed by flow cytometry after staining with FITC-conjugated anti-CD49b. (B) WNV infection of NK cell-depleted mice. Twenty mice were treated with either anti-NK1.1 or the isotype control (anti-SARS ORF7a) antibody and monitored for survival. No statistically significant differences in mortality were observed ($P > 0.1$).

Collectively, these experiments suggest that WNV-primed $CD8^+$ T cells control neuronal infection in vitro, in part, through perforin-dependent mechanisms.

DISCUSSION

Previously, two groups independently demonstrated that $CD8^+$ T cells have an essential role in eradicating WNV from infected tissues in the periphery and CNS (55, 63). Nonetheless, the mechanism of clearance remained uncertain as $CD8^+$ T cells may use distinct pathways to control viral infection. This question is especially relevant for viruses that infect neurons as cytolysis by $CD8^+$ T cells could cause significant injury to these nonregenerating cell populations. Using multiple experimental approaches, we investigated whether $CD8^+$ T cells use the pore-forming molecule perforin to control infection by a lineage I New York isolate of WNV. Congenic C57BL/6 mice that lack perforin had higher central nervous system viral burdens and increased mortality rates after WNV infection, and infectious virus was recovered from the CNS for several weeks in the few surviving perforin-deficient mice. Moreover, adoptive transfer of wild-type but not perforin-deficient WNV-primed $CD8^+$ T cells markedly reduced infection in the CNS and improved survival of CD8-deficient mice. $CD8^+$ T-cell-mediated clearance of WNV in the CNS was class I MHC dependent, as no beneficial effect was observed after transfer to K^b- × D^b-deficient mice. The in vivo results were largely recapitulated in vitro using wild-type and perforin-deficient $CD8^+$ T cells and congenic cortical neurons. Thus, despite the risk of immunopathogenesis, $CD8^+$ T cells utilize, in part, a
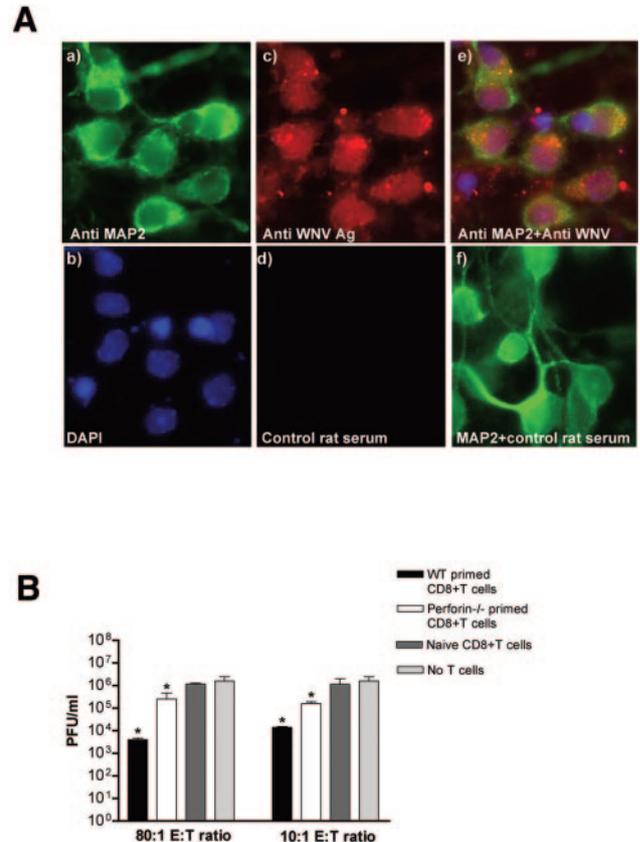

FIG. 6. $CD8^+$ T-cell-mediated control of WNV infection in primary cortical neurons. (A) Cortical neurons were infected with an MOI of 0.001 and 48 h later costained for neuronal and WNV antigen infection using naïve or WNV immune serum and an anti-MAP2 antibody. Purity of neuron cultures was assessed by comparing the MAP2 (a) and DAPI (b) staining. Infection of cells was evaluated after staining with WNV-immune (c) or WNV-naïve (d) rat serum. Infection of neurons was confirmed by merging the MAP2, anti-WNV, and DAPI images (e and f). (B) Clearance of WNV infection from neurons by $CD8^+$ T cells. One hour after WNV infection, purified naive or WNV-primed $CD8^+$ T cells from wild-type (WT) and perforin-deficient mice were added at an 80:1 or 10:1 E:T ratio. Supernatants were harvested 48 h later, and the reduction of WNV production was measured by plaque assay. Asterisks denote differences that are statistically significant ($P < 0.05$) compared to the addition of no $CD8^+$ T cells.

perforin-dependent, class I MHC-restricted mechanism to clear WNV from infected neurons.

An absence of perforin resulted in increased and sustained WNV infection in both peripheral and CNS tissues, data that are consistent with our previous findings for CD8-deficient mice (55). In the spleen, mice that lacked perforin did not efficiently clear infectious virus during the course of infection. Adoptive transfer of wild-type but not perforin-deficient WNV-primed $CD8^+$ T cells, however, completely cleared infectious virus from the spleen. A markedly higher viral burden was also observed in the CNS of perforin-deficient mice, and adoptive transfer of perforin-sufficient $CD8^+$ T cells to CD8-deficient recipients had a significantly greater protective effect than perforin-deficient $CD8^+$ T cells. Importantly, depletion studies with anti-CD8 antibodies confirmed that WNV-primed

CD8$^+$ T cells mediated the viral clearance and improvement in phenotype.

Our survival and virologic experiments suggest that a deficiency of perforin-expressing, cytolytic CD8$^+$ T cells has a detrimental effect after infection with a virulent lineage I New York WNV isolate. In contrast, another group showed a neutral or improved phenotype when perforin-deficient mice were infected with the lineage II Sarafend strain of WNV (64) or a prototype strain of the related Murray Valley encephalitis virus (36). Infection of perforin-deficient mice with WNV Sarafend had no effect on the survival rate, mean survival time, or viral burden in the brain (64). Although this group concluded that perforin did not play a crucial role in the recovery from Sarafend infection, higher mortality and viral burden were demonstrated in perforin- × Fas ligand-deficient mice compared to mice with the individual genetic deficiencies. Moreover, increased mortality and viral burden after Sarafend infection were observed in granzyme A- and B-deficient mice, suggesting that defects in the cytolytic machinery of T cells impaired WNV clearance. Although it is difficult to directly compare our results from perforin-deficient mice with those of Wang et al. (63), the disparity could be due to differences in the route of inoculation (footpad versus intravenous) or, more likely, the viral strain. The Sarafend and New York 2000 strains differ significantly at the amino acid level (22% capsid, 6% prM, 10% E, 10% NS1, 16% NS2a, 4% NS2b, 5% NS3, 23% NS4a, 14% NS4b, and 7% NS5), which could affect the potential of each virus to induce death in neuronal subsets. For a virulent strain, perforin-dependent lysis of a small number of infected neurons may outweigh the risk of CNS dissemination with widespread cell death induced directly by the virus.

Our findings establish the importance of perforin-dependent cytolysis in preventing WNV persistence. WNV was recovered from the brains of the few surviving perforin-deficient mice for several weeks, results that parallel our findings with CD8-deficient mice (55). The failure of CD8-deficient mice to clear virus from infected neurons is consistent with the findings of other studies with neuroadapted Sindbis virus in which CD8$^+$ T cells were required for clearance of viral RNA from neurons (3, 4). In the case of Sindbis virus, infection of neurons was cleared primarily by noncytolytic mechanisms, including the secretion of IFN-γ by activated CD8$^+$ T cells (3–5, 26). In contrast, adoptive transfer of WNV-primed IFN-γ-deficient CD8$^+$ T cells completely controlled infection in the spleen and CNS. Consistent with this, we do not observe long-term WNV persistence in mice deficient for IFN-γ or IFN-γ receptor (B. Shrestha and M. Diamond, unpublished observations). Thus, the pathogenesis of persistent neuronal infection appears to be virus specific and may be a function of deficits in one of several immunologic variables. For WNV, activated CD8$^+$ T cells control persistence, in part, through a perforin-dependent, IFN-γ-independent mechanism. Our preliminary studies also indicate that significant phenotypic changes to the virus do not occur during long-term viral persistence in the CNS: WNV that was isolated from the brains of the few surviving CD8-deficient mice at day 35 after infection showed a normal level of neurovirulence when inoculated intracranially into wild-type mice (M. Samuel and M. Diamond, unpublished results).

Studies with neurotropic viruses and perforin-deficient mice suggest that the virus, the host genetic background, and the specific neuronal target cell may all affect the ability of the cellular immune system to control and clear virus from the CNS (3, 16). In many cases, neurons may be protected from CD8$^+$ T-cell-mediated lysis because they basally express few class I MHC molecules. However, because inflammatory stimuli increase class I MHC expression in certain neuron subpopulations (31, 43), some may become vulnerable to immune targeting by virus-specific CD8$^+$ T cells during the course of infection. Indeed, for many CNS infections, perforin-dependent cytolysis of neuronal cells by CD8$^+$ T cells has pathogenic consequences. Perforin-deficient mice develop less severe disease after infection with lymphocytic choriomeningitis virus (22, 23, 59) or mouse hepatitis virus (37). In contrast, infection of perforin-deficient mice with neurovirulent Sindbis virus did not affect morbidity (49). However, infection of perforin-deficient mice with Theiler's murine encephalomyelitis virus, a pathogen that infects microglial and glial cells, resulted in decreased viral clearance from the CNS and enhanced demyelinating disease (48). To our knowledge, our studies with a virulent strain of WNV, which infects predominantly neurons, provide the first example in which perforin-dependent CD8$^+$ T-cell-mediated clearance of virus from neurons has a net beneficial effect on viral burden, neurological disease, and outcome. This may occur because of the high cytopathic potential of WNV for neurons (56).

The display of surface class I MHC molecules by neurons and their recognition by activated CD8$^+$ T cells have remained controversial. In vitro studies suggested that sympathetic neurons in culture express functional levels of class I MHC molecules and are targets for antigen-restricted CD8$^+$ T-cell lysis (39). Recent studies with mice demonstrated very low levels of classical class I MHC antigens in neurons infected with Sindbis (26) or herpes simplex (47) viruses. Indeed, we have similarly observed low levels of class I MHC molecules on neurons infected with WNV in vitro (B. Shrestha and M. Diamond, unpublished results). Nonetheless, our experiments with K^b- × D^b-deficient mice suggest that the levels of class I MHC molecules are sufficient for antigen presentation and perforin-dependent death by activated CD8$^+$ T cells. Adoptive transfer of wild-type or perforin-deficient WNV-primed CD8$^+$ T cells did not clear virus from infected CNS neurons in K^b- × D^b-deficient mice. Because in theory CD8$^+$ T cells could control WNV infection indirectly after interacting with other class I MHC-expressing cells (e.g., microglia, astrocytes, or oligodendrocytes), in vitro experiments were performed with highly purified primary cortical neurons. Importantly, the presence of perforin in CD8$^+$ T cells enhanced the control of WNV infection in these neurons. Taken together, our in vitro and in vivo data suggest that WNV-primed CD8$^+$ T cells control infection in CNS neurons, in part, by a class I MHC-restricted and perforin-dependent mechanism.

Surprisingly, the antibody depletion studies suggest that NK cells do not have a significant role in perforin-dependent or -independent control of WNV infection in mice. Similarly, no significant difference in phenotype after WNV infection was observed in Ly49A transgenic mice (25), which lack functional circulating NK cells (M. Engle and M. Diamond, unpublished results). Moreover, and in contrast to that seen after dengue virus infection (53), we have not observed early activation of NK cells in the lymph node after WNV infection (E. Mehlhop and M. Diamond, unpublished results). Although it remains

unclear why NK cells do not contribute to protection against WNV in mice, some flaviviruses may evade NK cell cytotoxicity by increasing the surface expression of MHC class I molecules on infected cells (7, 27–29), effectively transmitting an inhibitory signal through intracellular tyrosine-based inhibitor motifs.

Studies with immunodeficient mice (2, 8, 10, 13, 14, 30, 51, 60–63) have helped to elucidate the mechanisms of pathogenesis and protection against WNV infection. Our data suggest that at least for the highly virulent lineage I New York WNV strain, CD8$^+$ T cells use perforin-dependent, class I MHC-restricted mechanisms to clear infection from neurons. Although recovery from WNV infection is associated with a risk of immunopathogenesis by CD8$^+$ T cells, attenuating these interactions with broad-spectrum immunosuppressive agents could have more devastating consequences.

REFERENCES

1. **Asnis, D. S., R. Conetta, A. A. Teixeira, G. Waldman, and B. A. Sampson.** 2000. The West Nile virus outbreak of 1999 in New York: the Flushing Hospital experience. Clin. Infect. Dis. **30:**413–418.
2. **Ben-Nathan, D., I. Huitinga, S. Lustig, N. van Rooijen, and D. Kobiler.** 1996. West Nile virus neuroinvasion and encephalitis induced by macrophage depletion in mice. Arch. Virol. **141:**459–469.
3. **Binder, G. K., and D. E. Griffin.** 2003. Immune-mediated clearance of virus from the central nervous system. Microbes Infect. **5:**439–448.
4. **Binder, G. K., and D. E. Griffin.** 2001. Interferon-gamma-mediated site-specific clearance of alphavirus from CNS neurons. Science **293:**303–306.
5. **Burdeinick-Kerr, R., and D. E. Griffin.** 2005. Gamma interferon-dependent, noncytolytic clearance of Sindbis virus infection from neurons in vitro. J. Virol. **79:**5374–5385.
6. **Byrne, S. N., G. M. Halliday, L. J. Johnston, and N. J. King.** 2001. Interleukin-1beta but not tumor necrosis factor is involved in West Nile virus-induced Langerhans cell migration from the skin in C57BL/6 mice. J. Investig. Dermatol. **117:**702–709.
7. **Diamond, M. S.** 2003. Evasion of innate and adaptive immunity by flaviviruses. Immunol. Cell Biol. **81:**196–206.
8. **Diamond, M. S., B. Shrestha, A. Marri, D. Mahan, and M. Engle.** 2003. B cells and antibody play critical roles in the immediate defense of disseminated infection by West Nile encephalitis virus. J. Virol. **77:**2578–2586.
9. **Diamond, M. S., B. Shrestha, E. Mehlhop, E. Sitati, and M. Engle.** 2003. Innate and adaptive immune responses determine protection against disseminated infection by West Nile encephalitis virus. Viral Immunol. **16:**259–278.
10. **Diamond, M. S., E. Sitati, L. Friend, B. Shrestha, S. Higgs, and M. Engle.** 2003. Induced IgM protects against lethal West Nile virus infection. J. Exp. Med. **198:**1–11.
11. **Eldadah, A. H., and N. Nathanson.** 1967. Pathogenesis of West Nile virus encephalitis in mice and rats. II. Virus multiplication, evolution of immunofluorescence, and development of histological lesions in the brain. Am. J. Epidemiol. **86:**776–790.
12. **Eldadah, A. H., N. Nathanson, and R. Sarsitis.** 1967. Pathogenesis of West Nile virus encephalitis in mice and rats. I. Influence of age and species on mortality and infection. Am. J. Epidemiol. **86:**765–775.
13. **Engle, M. J., and M. S. Diamond.** 2003. Antibody prophylaxis and therapy against West Nile virus infection in wild-type and immunodeficient mice. J. Virol. **77:**12941–12949.
14. **Halevy, M., Y. Akov, D. Ben-Nathan, D. Kobiler, B. Lachmi, and S. Lustig.** 1994. Loss of active neuroinvasiveness in attenuated strains of West Nile virus: pathogenicity in immunocompetent and SCID mice. Arch. Virol. **137:**355–370.
15. **Harty, J. T., and V. P. Badovinac.** 2002. Influence of effector molecules on the CD8(+) T cell response to infection. Curr. Opin. Immunol. **14:**360–365.
16. **Harty, J. T., A. R. Tvinnereim, and D. W. White.** 2000. CD8+ T cell effector mechanisms in resistance to infection. Annu. Rev. Immunol. **18:**275–308.
17. **Hill, A. B., A. Mullbacher, C. Parrish, G. Coia, E. G. Westaway, and R. V. Blanden.** 1992. Broad cross-reactivity with marked fine specificity in the cytotoxic T cell response to flaviviruses. J. Gen. Virol. **73:**1115–1123.
18. **Ho, L. J., J. J. Wang, M. F. Shaio, C. L. Kao, D. M. Chang, S. W. Han, and J. H. Lai.** 2001. Infection of human dendritic cells by dengue virus causes cell maturation and cytokine production. J. Immunol. **166:**1499–1506.
19. **Hubalek, Z., and J. Halouzka.** 1999. West Nile fever—a reemerging mosquito-borne viral disease in Europe. Emerg. Infect. Dis. **5:**643–650.
20. **Johnston, L. J., G. M. Halliday, and N. J. King.** 2000. Langerhans cells migrate to local lymph nodes following cutaneous infection with an arbovirus. J. Investig. Dermatol. **114:**560–568.
21. **Johnston, L. J., G. M. Halliday, and N. J. C. King.** 1996. Phenotypic changes in Langerhans' cells after infection with arboviruses: a role in the immune response to epidermally acquired viral infection? J. Virol. **70:**4761–4766.
22. **Kagi, D., B. Ledermann, K. Burki, P. Seiler, B. Odermatt, K. J. Olsen, E. R. Podack, R. M. Zinkernagel, and H. Hengartner.** 1994. Cytotoxicity mediated by T cells and natural killer cells is greatly impaired in perforin-deficient mice. Nature **369:**31–37.
23. **Kagi, D., F. Vignaux, B. Ledermann, K. Burki, V. Depraetere, S. Nagata, H. Hengartner, and P. Golstein.** 1994. Fas and perforin pathways as major mechanisms of T cell-mediated cytotoxicity. Science **265:**528–530.
24. **Kesson, A. M., R. V. Blanden, and A. Mullbacher.** 1987. The primary in vivo murine cytotoxic T cell response to the flavivirus, West Nile. J. Gen. Virol. **68:**2001–2006.
25. **Kim, S., K. Iizuka, H. L. Aguila, I. L. Weissman, and W. M. Yokoyama.** 2000. In vivo natural killer cell activities revealed by natural killer cell-deficient mice. Proc. Natl. Acad. Sci. USA **97:**2731–2736.
26. **Kimura, T., and D. E. Griffin.** 2000. Role of CD8$^+$ T cells and major histocompatibility complex class I expression in the central nervous system of mice infected with neurovirulent Sindbis virus. J. Virol. **74:**6117–6125.
27. **King, N. J., and A. M. Kesson.** 2003. Interaction of flaviviruses with cells of the vertebrate host and decoy of the immune response. Immunol. Cell Biol. **81:**207–216.
28. **King, N. J., and A. M. Kesson.** 1988. Interferon-independent increases in class I major histocompatibility complex antigen expression follow flavivirus infection. J. Gen. Virol. **69:**2535–2543.
29. **King, N. J., L. E. Maxwell, and A. M. Kesson.** 1989. Induction of class I major histocompatibility complex antigen expression by West Nile virus on gamma interferon-refractory early murine trophoblast cells. Proc. Natl. Acad. Sci. USA **86:**911–915.
30. **Klein, R. S., E. Lin, B. Zhang, A. D. Luster, J. Tollett, M. A. Samuel, M. Engle, and M. S. Diamond.** 2005. Neuronal CXCL10 directs CD8$^+$ T-cell recruitment and control of West Nile virus encephalitis. J. Virol. **79:**11457–11466.
31. **Lampson, L. A., and W. F. Hickey.** 1986. Monoclonal antibody analysis of MHC expression in human brain biopsies: tissue ranging from "histologically normal" to that showing different levels of glial tumor involvement. J. Immunol. **136:**4054–4062.
32. **Lanciotti, R. S., A. J. Kerst, R. S. Nasci, M. S. Godsey, C. J. Mitchell, H. M. Savage, N. Komar, N. A. Panella, B. C. Allen, K. E. Volpe, B. S. Davis, and J. T. Roehrig.** 2000. Rapid detection of West Nile virus from human clinical specimens, field-collected mosquitoes, and avian samples by a TaqMan reverse transcriptase-PCR assay. J. Clin. Microbiol. **38:**4066–4071.
33. **Leis, A. A., J. Fratkin, D. S. Stokic, T. Harrington, R. M. Webb, and S. A. Slavinski.** 2003. West Nile poliomyelitis. Lancet Infect. Dis. **3:**9–10.
34. **Leis, A. A., D. S. Stokic, J. L. Polk, V. Dostrow, and M. Winkelmann.** 2002. A poliomyelitis-like syndrome from West Nile virus infection. N. Engl. J. Med. **347:**1279–1280.
35. **Libraty, D. H., S. Pichyangkul, C. Ajariyakhajorn, T. P. Endy, and F. A. Ennis.** 2001. Human dendritic cells are activated by dengue virus infection: enhancement by gamma interferon and implications for disease pathogenesis. J. Virol. **75:**3501–3508.
36. **Licon Luna, R. M., E. Lee, A. Müllbacher, R. V. Blanden, R. Langman, and M. Lobigs.** 2002. Lack of both Fas ligand and perforin protects from flavivirus-mediated encephalitis in mice. J. Virol. **76:**3202–3211.
37. **Lin, M. T., S. A. Stohlman, and D. R. Hinton.** 1997. Mouse hepatitis virus is cleared from the central nervous systems of mice lacking perforin-mediated cytolysis. J. Virol. **71:**383–391.
38. **Lobigs, M., C. E. Arthur, A. Mullbacher, and R. V. Blanden.** 1994. The flavivirus nonstructural protein NS3 is a dominant source of cytotoxic T cell peptide determinants. Virology **202:**195–201.
39. **Manning, P. T., E. M. Johnson, Jr., C. L. Wilcox, M. A. Palmatier, and J. H. Russell.** 1987. MHC-specific cytotoxic T lymphocyte killing of dissociated sympathetic neuronal cultures. Am. J. Pathol. **128:**395–409.
40. **Marovich, M., G. Grouard-Vogel, M. Louder, M. Eller, W. Sun, S. J. Wu, R. Putvatana, G. Murphy, B. Tassaneetrithep, T. Burgess, D. Birx, C. Hayes, S. Schlesinger-Frankel, and J. Mascola.** 2001. Human dendritic cells as targets of dengue virus infection. J. Investig. Dermatol. Symp. Proc. **6:**219–224.
41. **McClellan, J. S., S. A. Tibbetts, S. Gangappa, K. A. Brett, and H. W. Virgin IV.** 2004. Critical role of CD4 T cells in an antibody-independent mechanism of vaccination against gammaherpesvirus latency. J. Virol. **78:**6836–6845.

42. **Medana, I. M., A. Gallimore, A. Oxenius, M. M. Martinic, H. Wekerle, and H. Neumann.** 2000. MHC class I-restricted killing of neurons by virus-specific CD8+ T lymphocytes is effected through the Fas/FasL, but not the perforin pathway. Eur. J. Immunol. **30:**3623–3633.

43. **Mucke, L., and M. B. Oldstone.** 1992. The expression of major histocompatibility complex (MHC) class I antigens in the brain differs markedly in acute and persistent infections with lymphocytic choriomeningitis virus (LCMV). J. Neuroimmunol. **36:**193–198.

44. **Nelson, C. A., A. Pekosz, C. A. Lee, M. S. Diamond, and D. H. Fremont.** 2005. Structure and intracellular targeting of the ORF7a protein of SARS-associated coronavirus. Structure **13:**75–85.

45. **Ng, M. L., J. Howe, V. Sreenivasan, and J. J. Mulders.** 1994. Flavivirus West Nile (Sarafend) egress at the plasma membrane. Arch. Virol. **137:**303–313.

46. **Perarnau, B., M. F. Saron, B. R. San Martin, N. Bervas, H. Ong, M. J. Soloski, A. G. Smith, J. M. Ure, J. E. Gairin, and F. A. Lemonnier.** 1999. Single H2Kb, H2Db and double H2KbDb knockout mice: peripheral CD8+ T cell repertoire and anti-lymphocytic choriomeningitis virus cytolytic responses. Eur. J. Immunol. **29:**1243–1252.

47. **Pereira, R. A., and A. Simmons.** 1999. Cell surface expression of H2 antigens on primary sensory neurons in response to acute but not latent herpes simplex virus infection in vivo. J. Virol. **73:**6484–6489.

48. **Rossi, C. P., A. McAllister, M. Tanguy, D. Kägi, and M. Brahic.** 1998. Theiler's virus infection of perforin-deficient mice. J. Virol. **72:**4515–4519.

49. **Rowell, J. F., and D. E. Griffin.** 2002. Contribution of T cells to mortality in neurovirulent Sindbis virus encephalomyelitis. J. Neuroimmunol. **127:**106–114.

50. **Russell, J. H., and T. J. Ley.** 2002. Lymphocyte-mediated cytotoxicity. Annu. Rev. Immunol. **20:**323–370.

51. **Samuel, M. A., and M. S. Diamond.** 2005. Alpha/beta IFN protects against lethal West Nile virus infection by restricting cellular tropism and enhancing neuronal survival. J. Virol. **79:**13350–13361.

52. **Scherret, J. H., M. Poidinger, J. S. Mackenzie, A. K. Broom, V. Deubel, W. I. Lipkin, T. Briese, E. A. Gould, and R. A. Hall.** 2001. The relationships between West Nile and Kunjin viruses. Emerg. Infect. Dis. **7:**697–705.

53. **Shresta, S., J. L. Kyle, P. Robert Beatty, and E. Harris.** 2004. Early activation of natural killer and B cells in response to primary dengue virus infection in A/J mice. Virology **319:**262–273.

54. **Shresta, S., C. T. Pham, D. A. Thomas, T. A. Graubert, and T. J. Ley.** 1998. How do cytotoxic lymphocytes kill their targets? Curr. Opin. Immunol. **10:**581–587.

55. **Shrestha, B., and M. S. Diamond.** 2004. Role of CD8+ T cells in control of West Nile virus infection. J. Virol. **78:**8312–8321.

56. **Shrestha, B., D. Gottlieb, and M. S. Diamond.** 2003. Infection and injury of neurons by West Nile encephalitis virus. J. Virol. **77:**13203–13213.

57. **Steele, K. E., M. J. Linn, R. J. Schoepp, N. Komar, T. W. Geisbert, R. M. Manduca, P. P. Calle, B. L. Raphael, T. L. Clippinger, T. Larsen, J. Smith, R. S. Lanciotti, N. A. Panella, and T. S. McNamara.** 2000. Pathology of fatal West Nile virus infections in native and exotic birds during the 1999 outbreak in New York City, New York. Vet. Pathol. **37:**208–224.

58. **Tsai, T. F., F. Popovici, C. Cernescu, G. L. Campbell, and N. I. Nedelcu.** 1998. West Nile encephalitis epidemic in southeastern Romania. Lancet **352:**767–771.

59. **Walsh, C. M., M. Matloubian, C. C. Liu, R. Ueda, C. G. Kurahara, J. L. Christensen, M. T. Huang, J. D. Young, R. Ahmed, and W. R. Clark.** 1994. Immune function in mice lacking the perforin gene. Proc. Natl. Acad. Sci. USA **91:**10854–10858.

60. **Wang, T., and E. Fikrig.** 2004. Immunity to West Nile virus. Curr. Opin. Immunol. **16:**519–523.

61. **Wang, T., E. Scully, Z. Yin, J. H. Kim, S. Wang, J. Yan, M. Mamula, J. F. Anderson, J. Craft, and E. Fikrig.** 2003. IFN-γ-producing γδ T cells help control murine West Nile virus infection. J. Immunol. **171:**2524–2531.

62. **Wang, T., T. Town, L. Alexopoulou, J. F. Anderson, E. Fikrig, and R. A. Flavell.** 2004. Toll-like receptor 3 mediates West Nile virus entry into the brain causing lethal encephalitis. Nat. Med. **10:**1366–1373.

63. **Wang, Y., M. Lobigs, E. Lee, and A. Müllbacher.** 2003. CD8+ T cells mediate recovery and immunopathology in West Nile virus encephalitis. J. Virol. **77:**13323–13334.

64. **Wang, Y., M. Lobigs, E. Lee, and A. Mullbacher.** 2004. Exocytosis and Fas mediated cytolytic mechanisms exert protection from West Nile virus induced encephalitis in mice. Immunol. Cell Biol. **82:**170–173.

65. **Weiner, L. P., G. A. Cole, and N. Nathanson.** 1970. Experimental encephalitis following peripheral inoculation of West Nile virus in mice of different ages. J. Hyg. (London) **68:**435–446.

66. **Wu, S. J., G. Grouard-Vogel, W. Sun, J. R. Mascola, E. Brachtel, R. Putvatana, M. K. Louder, L. Filgueira, M. A. Marovich, H. K. Wong, A. Blauvelt, G. S. Murphy, M. L. Robb, B. L. Innes, D. L. Birx, C. G. Hayes, and S. S. Frankel.** 2000. Human skin Langerhans cells are targets of dengue virus infection. Nat. Med. **6:**816–820.

67. **Xiao, S. Y., H. Guzman, H. Zhang, A. P. Travassos da Rosa, and R. B. Tesh.** 2001. West Nile virus infection in the golden hamster (Mesocricetus auratus): a model for West Nile encephalitis. Emerg. Infect. Dis. **7:**714–721.

68. **Zhang, B., J. Tanaka, L. Yang, M. Sakanaka, R. Hata, N. Maeda, and N. Mitsuda.** 2004. Protective effect of vitamin E against focal brain ischemia and neuronal death through induction of target genes of hypoxia-inducible factor-1. Neuroscience **126:**433–440.